Kinetics and Mechanism of Emulsion Copolymerization. IV. Kinetic Modeling of Emulsion Copolymerization of Styrene and Methyl Methacrylate

MAMORU NOMURA, ICHIRO HORIE, MASAYUKI KUBO, and KAZUMI FUJITA, *Department of Industrial Chemistry, Fukui University, Fukui, Japan*

Synopsis

Based on the micellar nucleation theory, a mathematical kinetic model for an unseeded emulsion copolymerization system is developed, where the radicals with and without electric charge are discriminated from each other in view of the role in the particle nucleation process. In order to demonstrate the validity and utility of this kinetic model, the experiments of the unseeded emulsion copolymerization of styrene (ST) and methyl methacrylate (MMA) are carried out varying the initial initiator (potassium persulfate) and emulsifier (sodium lauryl sulfate) concentrations and the monomer composition in the initial monomer feed, and various kinetic features observed are compared with the model predictions. It is concluded from this comparison that in this system, almost all the polymer particles are generated by the charged radicals stemming from the initiator, and further that this mathematical kinetic model can provide a satisfactory explanation of the various kinetic features observed.

INTRODUCTION

The present authors have developed a kinetic model for seeded emulsion copolymerizations by applying the so-called pseudohomopolymerization approach.[1-4] According to this model, conventional complex kinetic equations describing such emulsion copolymerization systems can be converted into very simple forms analogous to those of emulsion homopolymerization only by introducing mean rate coefficients. Recently, other researchers have proved that this kinetic model and approach are very useful in simplifying the mathematical treatment of emulsion copolymerization equations.[5,6] In previous articles,[2-4] we have analyzed the rate of seeded emulsion copolymerization of styrene (ST) and methyl methacrylate (MMA) using this kinetic model and succeeded in quantitatively explaining the effects of a number of factors affecting the rate of this seeded emulsion copolymerization system. Furthermore, we have also shown that the Smith-Ewart case II kinetic model does not apply to this system because of dominant radical desorption from the polymer particles. However, no further study on the kinetics and mechanisms of the unseeded system has been carried out.

*Correspondence should be directed to Mamoru Nomura, Department of Industrial Chemistry, Fukui University, Fukui, Japan.

Journal of Applied Polymer Science, Vol. 37, 1029–1050 (1989)
 CCC 0021-8995/89/041029-22$04.00

It has been demonstrated by the present authors[7] that the emulsifier micelle is the principal locus of particle formation in the emulsion copolymerization of ST and MMA except in the vicinity of the critical micellar concentration (CMC) by measuring the composition of copolymers produced in the very beginning of the reaction. In this report, therefore, a simulation model for the processes of particle nucleation and its growth will be developed first based on the micellar nucleation hypothesis, including the concept of radical capture efficiency of the micelles relative to the polymer particles,[8] the mechanism of radical desorption and reabsorption in the micelles and polymer particles,[9] and the knowledge of the particle growth mechanism obtained in our previous work of the seeded emulsion copolymerization of ST and MMA.[2-4] Then, the experimental observations on the number of polymer particles formed and the monomer conversion versus time history and composition of copolymers produced will be compared to the model predictions with varying the initial emulsifier and initiator concentrations and the initial monomer composition to demonstrate the validity and utility of the kinetic model developed in this study.

PARTICLE NUCLEATION AND GROWTH MODEL

Let us consider an emulsion copolymerization system where two monomers, ST and MMA, are copolymerized, and sodium lauryl sulfate and potassium persulfate are employed as emulsifier and initiator, respectively. Based on the micellar nucleation hypothesis, particle formation is assumed to take place according to the following mechanism: The radicals in the water phase enter the monomer-swollen micelles, initiate polymerization, and propagate to a certain chain length which is long enough not to escape out of the micelles. If such polymer radicals could continue growing further without termination or chain transfer to monomer, they would finally convert these micelles into the polymer particles. The radicals in the water phase are classified into two groups (Table I) in view of the role of the electrostatic interaction between the radical and the negatively charged emulsifier micelle in the process of particle formation. One is the negatively charged radicals, which consist of the initiator radicals (I_{1w}^*) and the oligomeric radicals produced by the initiation and propagation reactions between the initiator radicals and the dissolved monomers in the water phase (I_{sw}^*, I_{mw}^*). The other is the oligomeric radicals without charge, which are comprised mainly of monomer radicals produced by chain transfer to monomer in the polymer particles followed by desorption into the water phase (M_{sw}^*, M_{mw}^*). In this study, these two types of radicals are discriminated from each other in the process of particle formation because their efficiencies for particle nucleation would be different due to the difference in the electrostatic interaction between the radical and the micelle along with the difference in chemical and physical properties of respective radicals. The negatively charged radicals, when entering the micelles with negative charged surfaces, may be hindered because of the electrostatic forces of repulsion between them. However, such radicals, once they had entered the micelles through the electrostatic barrier at their surface, would be hindered in escaping out of the micelles by the surrounding electrostatic barrier. Therefore, one can expect that these radicals have sufficient time periods to

TABLE I
Elementary Reactions and Their Rates

Reaction scheme	Reaction rate
(1) Initiation by water-soluble initiator in the water phase	
$I \rightarrow 2I_w^*$	r_i
(2) Nucleation of polymer particles[a]	
(i) By entry of charged radicals into micelles	
$m_e + I_w^* \rightarrow N_I^*$	$k_{1I}[I^*]_w m_e$ (T − 1)
(ii) By entry of uncharged radicals into micelles	
$m_e + M_{sw}^* \rightarrow N_{os}^*$	$k_{1s}[M_s^*]_w m_e$ (T − 2)
$m_e + M_{mw}^* \rightarrow N_{om}^*$	$k_{1m}[M_m^*]_w m_e$ (T − 3)
(3) Entry of radicals into polymer particles	
(i) Instantaneous termination	
$N^* + I_w^* \rightarrow N_o$	$k_{2I}[I^*]_w N^*$ (T − 4)
$N^* + M_{sw}^* \rightarrow N_o$	$k_{2s}[M_s^*]_w N^*$ (T − 5)
$N^* + M_{mw}^* \rightarrow N_o$	$k_{2m}[M_m^*]_w N^*$ (T − 6)
(ii) Activation of dead particles	
$N_o + I_w^* \rightarrow N_I^*$	$k_{2I}[I^*]_w N_o$ (T − 7)
$N_o + M_{sw}^* \rightarrow N_{os}^*$	$k_{2s}[M_s^*]_w N_o$ (T − 8)
$N_o + M_{mw}^* \rightarrow N_{om}^*$	$k_{2m}[M_m^*]_w N_o$ (T − 9)
(4) Propagation in polymer particles	
$P_s^* + M_s \rightarrow P_s^*$	$k_{pss}[M_s]_p N_s^*$ (T − 10)
$P_s^* + M_m \rightarrow P_m^*$	$k_{psm}[M_m]_p N_s^*$ (T − 11)
$P_m^* + M_s \rightarrow P_s^*$	$k_{pms}[M_s]_p N_m^*$ (T − 12)
$P_m^* + M_m \rightarrow P_m^*$	$k_{pmm}[M_m]_p N_m^*$ (T − 13)
(5) Chain transfer to monomer in polymer particles	
$P_s^* + M_s \rightarrow P + M_s^*$	$k_{ss}[M_s]_p N_s^*$ (T − 14)
$P_s^* + M_m \rightarrow P + M_m^*$	$k_{sm}[M_m]_p N_s^*$ (T − 15)
$P_m^* + M_s \rightarrow P + M_s^*$	$k_{ms}[M_s]_p N_m^*$ (T − 16)
$P_m^* + M_m \rightarrow P + M_m^*$	$k_{mm}[M_m]_p N_m^*$ (T − 17)
(6) Desorption of radicals from polymer particles	
$N_{II}^* \rightarrow N_o + I_{Iw}^*$	$k_{fI} N_{II}^*$ (T − 18)
$N_s^* \rightarrow N_o + M_{sw}^*$	$k_{fs} N_s^*$ (T − 19)
$N_m^* \rightarrow N_o + M_{mw}^*$	$k_{fm} N_m^*$ (T − 20)

[a] $I_w^* = I_{Iw}^* + I_{sw}^* + I_{mw}^*$, $[I^*]_w = [I_I^*]_w + [I_s^*]_w + [I_m^*]_w$, $N_I^* = N_{II}^* + N_{Is}^* + N_{Im}^*$

initiate and propagate up to a longer chain length and hence have a higher possibility of converting the micelles into the polymer particles than those without charge. On the other hand, the uncharged radicals can be expected to enter the negatively charged micelles much easier than those with charge. However, if they are not so reactive, they can easily escape out of the micelles into the water phase before adding a number of monomer units and converting the micelles into polymer particles.

In developing a mathematical kinetic model for an unseeded emulsion copolymerization system according to the mechanism of particle nucleation assumed above, the following assumptions will be made for simplicity: (1) Each polymer particle and emulsifier micelle contains at most one radical; (2) instantaneous termination occurs when another radical enters the polymer particle and the micelle that already contain a radical; (3) propagation, termination and chain transfer reactions in the water phase take place only to a negligible extent from a kinetic point of view; (4) the radicals which can

desorb from the micelles and the polymer particles are mainly uncharged monomer radicals that are produced by chain transfer to monomer molecules.

In the next section, the basic kinetic equations for an unseeded emulsion copolymerization system will be developed.

Derivation of Basic Equations

Based on the mechanisms of particle nucleation and its growth and the assumptions referred to above, the following basic kinetic equations can be established using the rate expressions defined in Table I. For simplicity, the steady-state hypothesis is applied to the differential equations describing radical balance:

1. The rate of particle formation:

$$\frac{dN_T}{dt} = k_{1I}[I^*]_w m_e + k_{1s}[M_s^*]_w m_e + k_{1m}[M_m^*]m_e \tag{1}$$

where, N_T is the total number of polymer particles: k_{1j} ($j = I$, s, and m) is the apparent rate coefficient for radical entry into the micelles, which includes the effects of radical desorption and electrostatic interaction between a radical and a micelle; m_e is the concentration of emulsifier micelles; $[I^*]_w$ is the concentration of charged radicals with an initiator fragment at their ends; and $[M_s^*]_w$ and $[M_m^*]_w$ are the concentrations of uncharged ST and MMA radicals, respectively. Subscripts, I, s, m, and w denote the quantities relating to the initiator, ST, MMA, and the water phase, respectively. The first term of the right-hand side of Eq. (1) shows the rate of particle formation due to the charged radicals, and the second and third terms, due to ST and MMA oligomeric (monomer) radicals without charge, respectively. At steady state, the following balance equations for $[I^*]_w$, $[M_s^*]_w$, and $[M_m^*]_w$ can be established.

$$\frac{d[I^*]_w}{dt} = r_i + k_{fI}N_H^* - k_{2I}[I^*]_w N_T - k_{1I}[I^*]_w m_e - k_{twI}[I^*]_w[R^*]_w = 0 \tag{2}$$

$$\frac{d[M_s^*]_w}{dt} = k_{fs}N_s^* - k_{2s}[M_s^*]_w N_T - k_{1s}[M_s^*]_w m_e - k_{tws}[M_s^*]_w[R^*]_w = 0 \tag{3}$$

$$\frac{d[M_m^*]_w}{dt} = k_{fm}N_m^* - k_{2m}[M_m^*]_w N_T - k_{1m}[M_m^*]_w m_e - k_{twm}[M_m^*]_w[R^*]_w = 0 \tag{4}$$

where k_{2j} is the rate constant for radical entry into the polymer particles, k_{twj} is the mean rate constant for radical termination in the water phase involving the radical of j-species ($j = I$, s, m), and r_i is the rate of radical

production in the water phase given by

$$r_i = 2k_d f [I]_w \tag{5}$$

where k_d is the rate constant for initiator decomposition, f is the initiator efficiency, and $[I]_w$ is the initiator concentration in the water phase. Here k_{fj} is the rate coefficient for radical desorption from the polymer particles ($j = I, s, m$), and, for example, k_{fs}, the desorption rate coefficient for ST radicals is given by,[2]

$$k_{fs} = K_{0s}\left(\frac{\gamma_s C_{ss}[M_s]_p + C_{ms}[M_m]_p}{\gamma_s\{[M_s]_p + (K_{0s}\bar{n}_t/k_{pss})\} + [M_m]_p} \right) \tag{6a}$$

where γ_s is the reactivity ratio for ST monomer, C_{ms} is the chain transfer constant of MMA radicals to ST monomer molecules, and K_{os} represents the desorption rate constant for ST monomer radicals and is given by

$$K_{os} = \frac{12 D_{ws}\delta_s}{m_{ds} d_p^2} = \frac{7.8 D_{ws}\delta_s}{m_{ds} v_p^{2/3}} \tag{6b}$$

$$\delta_s = \left(1 + \frac{D_{ws}}{m_{ds} D_{ps}}\right)^{-1} \tag{6c}$$

where m_{ds} is the partition coefficient for ST monomer radicals between the water and particle phases, d_p and v_p are the average diameter and volume of polymer particles, respectively, and D_{ws} and D_{ps} are the diffusion coefficients for ST monomer radicals in the water and polymer particle phases, respectively. Here δ_s is the ratio of the water side to overall mass-transfer resistances for ST monomer radicals in the process of radical desorption from the polymer particles into the water phase. Here, N_I^* denotes the number of active polymer particles containing a charged radical with an initiator fragment at its end. N_s^* and N_m^* are the numbers of polymer particles containing ST and MMA radicals with and without charge, respectively, and are given by

$$N_I^* = N_{II}^* + N_{Is}^* + N_{Im}^* \tag{7a}$$

$$N_s^* = N_{os}^* + N_{Is}^* \tag{7b}$$

$$N_m^* = N_{om}^* + N_{Im}^* \tag{7c}$$

where, for example, N_{II}^*, N_{Is}^*, and N_{os}^* are the numbers of active polymer particles containing an initiator radical, a charged ST radical with an initiator fragment at its end and an uncharged ST radical, respectively. Furthermore, $[R^*]_w$ denotes the total concentration of radicals in the water phase and is given by

$$[R^*]_w = [I^*]_w + [M_s^*]_w + [M_m^*]_w \tag{8}$$

Considering the assumption that radical termination in the water phase can be neglected under usual conditions, Eqs. (2)–(4) lead to:

$$[I^*]_w = \frac{r_i + k_{fI}N_{II}^*}{k_{1I}m_e + k_{2I}N_T} \tag{2'}$$

$$[M_s^*]_w = \frac{k_{fs}N_s^*}{k_{1s}m_e + k_{2s}N_T} \tag{3'}$$

$$[M_m^*]_w = \frac{k_{fm}N_m^*}{k_{1m}m_e + k_{2m}N_T} \tag{4'}$$

Substitution of Eqs. (2')–(4') into Eq. (1) and rearrangement yields:

$$\frac{dN_T}{dt} = \frac{\epsilon_I S_M(r_i + k_{fI}N_{II}^*)}{\epsilon_I S_M + N_T} + \frac{\epsilon_s S_M k_{fs}N_s^*}{\epsilon_s S_M + N_T} + \frac{\epsilon_m S_M k_{fm}N_m^*}{\epsilon_m S_M + N_T} \tag{9}$$

where,

$$S_M = A_n m_e \tag{10}$$

$$\epsilon_j = (k_{1j}/k_{2j}A_n), (j = I, s, m) \tag{11}$$

Here S_M is the concentration of emulsifier forming micelles, A_n is the number of emulsifier molecules per micelle, and ϵ_j is the parameter that represents the radical capture efficiency of micelles relative to polymer particles for the radicals of j species.[8] At the present stage, however, it is actually impossible to predict the exact value of ϵ_j since only rough values of k_{1j} and k_{2j} can be evaluated theoretically,[9,10] and hence, the value of ϵ_j must be determined experimentally.

2. The number of polymer particles containing a radical of j species, N_j^*: N_{II}^*, N_s^*, and N_m^* can be related to the total number of active particles, N^*. Since N_{II}^* is far smaller than N_s^* and N_m^* because the initiator radical is so reactive that it is immediately transformed into ST or MMA radicals by adding monomer units even if it enters directly into the micelles, we have

$$N^* = N_{II}^* + N_s^* + N_m^* \simeq N_s^* + N_m^* \tag{12}$$

According to the results of the previous article,[2] the following relationship holds approximately at steady state,

$$(k_{psm} + k_{sm})[M_m]_p N_s^* = (k_{pms} + k_{ms})[M_s]_p N_m^* \tag{13}$$

where, for example, k_{psm} is the cross propagation rate constant of ST radicals to MMA monomer and k_{sm} is the cross chain transfer rate constant of ST radicals to MMA monomer. Considering that the value of k_{pij} is much greater than the value of k_{ij}, we define a new parameter, H_s, by rewriting Eq. (13),

as:

$$H_s = \frac{N_s^*}{N_s^* + N_m^*} = \frac{N_s^*}{N^*} = \left(\frac{k_{pmm}[M_s]_p \gamma_s}{k_{pss}[M_m]_p \gamma_m + k_{pmm}[M_s]_p \gamma_s} \right) \tag{14}$$

Using eqs. (12) and (14), N_s^* and N_m^* can be related to N^* as follows:

$$N_s^* = H_s N^* = \left(\frac{k_{pmm}[M_s]_p \gamma_s}{k_{pss}[M_m]_p \gamma_m + k_{pmm}[M_s]_p \gamma_s} \right) N^* \tag{15a}$$

$$N_m^* = (1 - H_s) N^* = \left(\frac{k_{pss}[M_m]_p \gamma_m}{k_{pss}[M_m]_p \gamma_m + k_{pmm}[M_s]_p \gamma_s} \right) N^* \tag{15b}$$

3. The total number of active polymer particles, N^*: The rate of increase in the total number of active polymer particles containing a radical, N^*, can be expressed by

$$\begin{aligned} \frac{dN^*}{dt} &= (k_{1I}[I^*]_w + k_{1s}[M_s^*]_w + k_{1m}[M_m^*]_w) m_e \\ &\quad + (k_{2I}[I^*]_w + k_{2s}[M_s^*]_w + k_{2m}[M_m^*]_w)(N_o - N^*) \\ &\quad - (k_{fI} N_{II}^* + k_{fs} N_s^* + k_{fm} N_m^*) \end{aligned} \tag{16}$$

where N_o is the number of dead polymer particles containing no radicals. Substituting Eqs. (2′), (3′), and (4′) into Eq. (16) yields:

$$\begin{aligned} \frac{dN^*}{dt} &= \left(\frac{\epsilon_I S_M + (N_T - 2N^*)}{\epsilon_I S_M + N_T} \right) (r_i + k_{fI} N_{II}^*) \\ &\quad + \left(\frac{\epsilon_s S_M + (N_T - 2N^*)}{\epsilon_s S_M + N_T} \right) (k_{fs} N_s^*) \\ &\quad + \left(\frac{\epsilon_m S_M + (N_T - 2N^*)}{\epsilon_m S_M + N_T} \right) (k_{fm} N_m^*) - (k_{fI} N_{II}^* + k_{fs} N_s^* + k_{fm} N_m^*) \end{aligned} \tag{17}$$

4. The rate of copolymerization, r_{ps}, r_{pm}, and r_{pt}: The rates of copolymerization for ST and MMA monomers, r_{ps} and r_{pm} are, respectively, expressed by

$$r_{ps} = M_{os} \left(\frac{dX_s}{dt} \right) = k_{pss}[M_s]_p N_s^* + k_{pms}[M_s]_p N_m^* \tag{18a}$$

$$r_{pm} = M_{om} \left(\frac{dX_m}{dt} \right) = k_{pmm}[M_m]_p N_m^* + k_{psm}[M_m]_p N_s^* \tag{18b}$$

and therefore, the total rate of copolymerization, r_{pt} is given by

$$r_{pt} = M_{ot}\left(\frac{dX_{Mt}}{dt}\right) = r_{ps} + r_{pm} \tag{19a}$$

where M_{os} and M_{om} denote the amounts of ST and of MMA monomers initially charged per unit volume of water, respectively, M_{ot} is the total amount of monomers initially charged ($M_{ot} = M_{os} + M_{om}$), and X_s and X_m are the conversions of ST and MMA monomers, respectively. X_{Mt} represents the total monomer conversion and is defined by

$$X_{Mt} = \frac{M_{os}X_s + M_{om}X_m}{M_{ot}} \tag{19b}$$

5. Balance on the emulsifier that forms micelles, S_M: The concentration of emulsifier forming micelles, S_M, decreases gradually with the progress of polymerization during the interval of particle formation, due to break up and absorption of their molecules onto the surfaces of growing polymer particles. Provided that the emulsifier molecules are adsorbed in a monomolecular layer on the surface of polymer particle and that the dissociation of emulsifier micelles and the adsorption of emulsifier molecules are very rapid compared with other rate processes, the following steady-state balance equation on the emulsifier forming micelles may be established with a good approximation.[8]

$$S_M = S_o - S_{cmc} - \left(36\pi V_p^2/\bar{a}^3\right)^{1/3} N_T^{1/3} \tag{20a}$$

where S_o is the concentration of emulsifier initially charged, S_{cmc} is the critical micellar concentration and V_p is the total volume of polymer particles per unit volume of water. If the volume of each component in the polymer particles can be assumed to be additive, V_p is expressed by

$$V_p = v_p N_T = \frac{M_{sp}}{\rho_s} + \frac{M_{mp}}{\rho_m} + \frac{M_{ot}X_{Mt}}{\rho_p} \tag{20b}$$

where M_{sp} is the amount of ST monomer absorbed in the polymer particles per unit volume of water, ρ_s is the density of ST monomer and ρ_p is the average density of the copolymer. Furthermore, $\bar{a}$ in Eq. (20a) represents the adsorption area of the emulsifier molecule on the surface of the copolymer particle and is assumed to be correlated approximately by

$$\bar{a} = a_s\Phi_s + a_m(1 - \Phi_s) \tag{20c}$$

where a_s and a_m are the adsorption areas of the emulsifier molecules in the emulsion homopolymerizations of ST and of MMA, respectively. Here Φ_s denotes the mole fraction of ST monomer units at the surface of monomer-swollen copolymer particle. If M_{os}, M_{sp}, and so on are expressed in g/cm^3 water, the approximate value of Φ_s may be evaluated, at least during the

interval of particle formation, from

$$\Phi_s = \frac{(M_{sp} + M_{os}X_s)/M_{ws}}{(M_{sp} + M_{os}X_s)/M_{ws} + (M_{mp} + M_{om}X_m)/M_{wm}} \tag{20d}$$

where M_{ws} and M_{wm} are the molecular weights of ST and MMA monomers, respectively.

6. Copolymer Composition, y_s and Y_s: For example, the instantaneous copolymer composition, y_s, the fraction of ST monomer units in the copolymers produced instantaneously is expressed, using Eqs. (18a') and (18b'), by

$$y_s = \frac{M_{os}dX_s}{M_{os}dX_s + M_{om}dX_m} = \frac{r_{ps}}{r_{ps} + r_{pm}} = \frac{r_{ps}}{r_{pt}} \tag{21}$$

On the other hand, the cumulative copolymer composition, Y_s, is expressed by

$$Y_s = \frac{M_{os}X_s}{M_{os}X_s + M_{om}X_m} = \frac{M_{os}X_s}{M_{ot}X_{Mt}} \tag{22}$$

Prediction of Monomer Concentration in Polymer Particle

In order to predict the progress of emulsion copolymerization by calculation using the mathematical kinetic model developed in the preceding section, it is essential for the concentration of each monomer in the polymer particles, $[M_s]_p$ and $[M_m]_p$, to be expressed as a function of either the reaction time or the monomer conversions. To date, two approaches have been proposed for predicting the monomer concentrations in the polymer particles. One is the thermodynamic approach applied first by Morton et al.[11] to an emulsion homopolymerization system and later extended by Guillot[12] to an emulsion copolymerization system. The other is an empirical method such as developed by the present authors.[4] Although the thermodynamic approach is indeed very fundamental and promising, we use here the empirical method developed by the present authors because the thermodynamic approach involves many parameters the values of which are not necessarily available.

When the solubility of each monomer in water is negligible, the mass balance equation on each monomer can be expressed, respectively, by

$$M_{os} = M_{os}X_s + M_{sp} + M_{sd} \tag{23a}$$

$$M_{om} = M_{om}X_m + M_{mp} + M_{md} \tag{23b}$$

where, for example, M_{sd} denotes the amount of ST monomer in the monomer droplets per unit volume of water. If the volume of each component in the polymer particles can be assumed to be additive and furthermore, M_{os}, M_{sp}, M_{sd} and so on are expressed in g/cm^3 water, the concentration of each monomer in the polymer particles, $[M_s]_p$ and $[M_m]_p$, can be represented

in mol/dm^3 particles, as follows:

$$[M_s]_p = \left(\frac{M_{sp}}{M_{sp}/\rho_s + M_{mp}/\rho_m + M_{ot}X_{Mt}/\rho_p}\right)\left(\frac{10^3}{M_{ws}}\right) \tag{24a}$$

$$[M_m]_p = \left(\frac{M_{mp}}{M_{sp}/\rho_s + M_{mp}/\rho_m + M_{ot}X_{Mt}/\rho_p}\right)\left(\frac{10^3}{M_{wm}}\right) \tag{24b}$$

where ρ_s is the density of ST monomer in g/cm^3 and ρ_p is the average density of the copolymer in g/cm^3. On the other hand, when the concentration of each monomer in the polymer particles is known, the amount of each monomer absorbed in the polymer particles per unit volume of water, M_{sp} and M_{mp}, can be calculated by the following equations which are obtained by solving Eqs. (24a) and (24b) simultaneously.

$$M_{sp} = \left(\frac{[M_s]_p M_{ws}}{1000 - [M_s]_p(M_{ws}/\rho_s) - [M_m]_p(M_{wm}/\rho_m)}\right)\left(\frac{M_{ot}X_{Mt}}{\rho_p}\right) \tag{25a}$$

$$M_{mp} = \left(\frac{[M_m]_p M_{wm}}{1000 - [M_s]_p(M_{ws}/\rho_s) - [M_m]_p(M_{wm}/\rho_m)}\right)\left(\frac{M_{ot}X_{Mt}}{\rho_p}\right) \tag{25b}$$

1. In the region where monomer droplets exist in the water phase: In the emulsion copolymerization of ST and MMA monomers, it was demonstrated that in this region, the concentration of each monomer in the polymer particles could be represented by the following empirical equations.[2]

$$[M_s]_p = 22.4\left(\frac{1 - F_{md}}{4 - F_{md}}\right) \tag{26a}$$

$$[M_m]_p = 27.6\left(\frac{F_{md}}{5 - F_{md}}\right) \tag{26b}$$

where F_{md} denotes the weight fraction of MMA in the monomer droplets which are in equilibrium with the monomer-swollen copolymer particles. It was also demonstrated experimentally that F_{md} was approximately equal to F_{mp}, the weight fraction of MMA monomer in the polymer particles.[4] Based on this experimental result, we have

$$F_{md} = \frac{M_{md}}{M_{sd} + M_{md}} = F_{mp} = \frac{M_{mp}}{M_{sp} + M_{mp}} = \frac{M_{md} + M_{mp}}{M_{sd} + M_{sp} + M_{md} + M_{mp}}$$

$$= \frac{M_{om}(1 - X_m)}{M_{ot}(1 - X_{Mt})} \tag{27}$$

Thus, by using Eqs. (26) and (27), the concentrations of ST and MMA

monomers in the polymer particles can be expressed as a function of monomer conversions in the region where monomer droplets exist in the water phase.

2. In the region where no monomer droplets exist in the water phase: In the region where the monomer droplets have disappeared from the water phase, it holds that $M_{sd} = M_{md} = 0$. Therefore, Eq. (23) can be modified to

$$M_{sp} = M_{os}(1 - X_s) \tag{28a}$$

$$M_{mp} = M_{om}(1 - X_m) \tag{28b}$$

By introducing Eq. (28) into Eq. (24), we can express the concentration of each monomer in the polymer particles as a function of the monomer conversions in this region.

3. The critical conversions where monomer droplets just disappear: The critical conversions where monomer droplets just disappear from the water phase, X_{sc} and X_{mc}, can be easily estimated by using Eqs. (23), (25), (26), and (27) as follows: When monomer droplets still exist in the water phase, the following inequalities derived from Eq. (23) must be satisfied.

$$M_{sd} = M_{os}(1 - X_s) - M_{sp} > 0 \tag{29a}$$

$$M_{md} = M_{om}(1 - X_m) - M_{mp} > 0 \tag{29b}$$

First, we evaluate the values of M_{sp} and M_{mp} using eqs. (25), (26), and (27) at the conversion of each monomer under consideration and then, calculate the values of M_{sd} and M_{md} by substituting the values of M_{sp} and M_{mp} and the conversion of each monomer into Eq. (29). If the values of M_{sd} and M_{md} thus obtained are both positive, the reaction is regarded to be still in the region where monomer droplets exist. Thus, we can determine the critical conversions by examining the values of M_{sd} and M_{md}.

Simplification of the Basic Equations

In this kinetic model, the parameters ϵ_m, ϵ_s, and ϵ_I are most important because the rate of particle formation is greatly affected by the values of these parameters. As is clear from the definition given by Eq. (11), it is reasonable to consider that the values of ϵ_s, ϵ_m, and ϵ_I would be different from each other because the parameter ϵ is a complicated function of the comonomer composition in the system; the electrostatic interaction between a radical and a micelle; and the water solubility, reactivity, and other physical and chemical properties of each radical. Since the values of these parameters cannot be predicted theoretically at the present stage, we have to determine these values experimentally. Therefore, we introduce here the assumption that the value of ϵ_s is approximately equal to that of ϵ_m so that we can easily determine the values of ϵ_s, ϵ_m, and ϵ_I.

$$\epsilon = \epsilon_s = \epsilon_m \tag{30}$$

Furthermore, we neglect the term $k_{fI}N_I^*$ in Eqs. (9) and (17) because the initiator radical would rather initiate polymerization than escape out of the

micelle due to its high reactivity and the electrostatic hindrance against desorption, as mentioned previously. For further simplification, the mean rate coefficient for radical desorption defined below is introduced.[2]

$$k_f N^* = k_{fs} N_s^* + k_{fm} N_m^* \tag{31}$$

By introducing Eq. (15) into Eq. (31), we have

$$k_f = \left(\frac{k_{fs} k_{pmm} [M_s]_p \gamma_s + k_{fm} k_{pss} [M_m]_p \gamma_m}{k_{pmm} [M_s]_p \gamma_s + k_{pss} [M_m]_p \gamma_m} \right) \tag{32}$$

As the results of the above assumptions and the introduction of a new parameter, ϵ, Eqs. (9) and (17) are simplified as follows:

$$\frac{dN_T}{dt} = r_i \left(\frac{\epsilon_I S_M}{\epsilon_I S_M + N_T} \right) + \left(\frac{\epsilon S_M}{\epsilon S_M + N_T} \right) k_f N^* \tag{9'}$$

$$\frac{dN^*}{dt} = r_i \left(\frac{\epsilon_I S_M + (N_T - 2N^*)}{\epsilon_I S_M + N_T} \right) - \left(\frac{2N^*}{\epsilon S_M + N_T} \right) k_f N^* \tag{17'}$$

If M_{os} and M_{om} are expressed in g/cm^3 water, Eq. (18) for copolymerization rates are also simplified as

$$\frac{dX_s}{dt} = \left(\frac{M_{ws}}{M_{os} N_A} \right) \left[k_{pss} H_s + k_{pms} (1 - H_s) \right] [M_s]_p N^* \tag{18a'}$$

$$\frac{dX_m}{dt} = \left(\frac{M_{wm}}{M_{om} N_A} \right) \left[k_{psm} H_s + k_{pmm} (1 - H_s) \right] [M_m]_p N^* \tag{18b'}$$

where N_A is the Avogadro's number.

Thus, we can predict the progress of copolymerization by solving a set of differential equations, Eqs. (9'), (17'), and (18') along with Eqs. (20) and (23)–(29). The simultaneous differential equations mentioned above were solved numerically on a digital computer. Comparisons between the model predictions and the experimental results will be made in the next section.

EXPERIMENTAL RESULTS AND MODEL PREDICTIONS

Commercially available MMA monomer inhibited with hydroquinone was first washed with saturated $NaHSO_3$ solution and then with 5% NaOH solution, while ST monomer of commerical grade was washed with 15% KOH to remove inhibitor. The monomers thus treated were washed further with deionized water, distilled twice under reduced nitrogen pressure, and stored at -20°C in a refrigerator. Postassium persulfate and sodium lauryl sulfate of extra pure grade was used as initiator and emulsifier, respectively, without further purification. All water used was purified by distillation in the presence of alkaline potassium permanganate.

The unseeded emulsion copolymerization of ST and MMA was carried out using the same experimental apparatus as shown previously.[13] The reactor

was a 400 cm^3 cylindrical glass vessel with a dished bottom, equipped with a four-blade paddle-type impeller. Four baffle plates made of stainless steel were set on the vessel wall at 90° intervals to improve mixing of the reaction mixture. The reactor vessel was charged with the desired amounts of monomers, emulsifier, and purified water, a small portion of which was put aside for preparing an aqueous initiator solution. The oxygen dissolved in the reaction mixture was purged by bubbling pure nitrogen gas (purity > 99.995%) through the reaction mixture for about 30 min from the sampling cock attached to the bottom of the reaction vessel. The polymerization was started by injecting the aqueous initiator solution, which had been prepared previously and deoxygenized with this pure nitrogen gas, from a dropping funnel into the reaction mixture. All the copolymerizations were carried out at 50 ± 0.5°C with the use of a thermostated water bath and under the atmosphere of this pure nitrogen gas. Impeller speeds were kept constant at 400 rpm. Total monomer conversion was determined gravimetrically. The copolymers were precipitated with methanol and filtered off with a glass crucible. The conversion of each monomer was determined by measuring the content of each monomer in the filtrate obtained above by gas chromatography with the same procedure as shown later.

The number of polymer particles produced was determined using Eq. (33)

$$N_T = \frac{6M_{ot}X_{Mt}}{\pi \bar{d}_p^3 \rho_p} \tag{33}$$

where X_{Mt} is the total monomer conversion and $\bar{d}_p$ is the volume average diameter of the particles defined by Eq. (34). The particle diameter was measured by electron microscopy.

$$\bar{d}_p = \left(\frac{\Sigma n_i d_{pi}^3}{\Sigma n_i} \right)^{1/3} \tag{34}$$

Further, the concentration of each monomer in the monomer-swollen polymer particles was measured by the following procedure to compare with the model predictions: The monomer droplets in the samples withdrawn from the sampling cock were immediately separated as a monomer layer with a centrifuge. A fraction of the aqueous phase under the monomer layer which contained only the monomer-swollen polymer particles was taken out with a syringe and poured into excess methanol. The precipitated copolymers were filtered off with a glass crucible and the filtrate was subjected to the measurement of monomer content by gas chromatography. In calculating the concentration of each monomer in the monomer-swollen polymer particles, the volume of each monomer and copolymer in the particles were assumed to be additive.

Comparison of Model Predictions with Experimental Results

Numerical Constants

The numerical values of constants at 50°C used in this study are listed in Table II. Most of them were cited from our previous article.[2] The values of

TABLE II
Numerical Values of Constants Used (50°C)

Constant	Units	Styrene(s)	Methyl methacrylate
k_p	dm^3/mol.s	210	650
γ	—	0.52	0.46
δ	—	0.16	0.16
C	—	1.2×10^{-5} (C_{ss})	2.0×10^{-5} (C_{mm})
		5.0×10^{-5} (C_{sm})	5.0×10^{-5} (C_{ms})
a	cm^2/molecule	35×10^{-16}	90×10^{-16}
D_w	cm^2/s	1.2×10^{-5}	1.7×10^{-5}
m_d	—	1300	50
ρ	g/cm^3	0.88	0.92
S_{cmc}	g/dm^3-water	0.50	
ρ_p	g/cm^3	1.1	
$k_d f$	1/s	6.7×10^{-7}	———

D_w, shown here, are the diffusion coefficients for ST and MMA monomer molecules, respectively, because it was assumed that the radicals that can desorb from and reenter the micelles and polymer particles are mostly monomer radicals. Concerning the value of δ_m, it should be noted here that in the range where the mole fraction of MMA in the initial monomer feed (F_{om}) is higher than 0.6, the value of δ_m decreases very sharply with an increase in the value of F_{om} according to the following approximate equation.[2]

$$\delta_m = 0.37 - 0.35F_{om} \qquad (F_{om} > 0.6) \tag{35}$$

The applicability of Eq. (20c) to the emulsion copolymerization of ST and MMA was ascertained experimentally, as shown in Figure 1, where the adsorption area, $\bar{a}$, of NaLS emulsifier was measured for various copolymer latex samples with known copolymer composition by applying the soap-titration method, plotted against the value of Φ_s and compared with the theoreti-

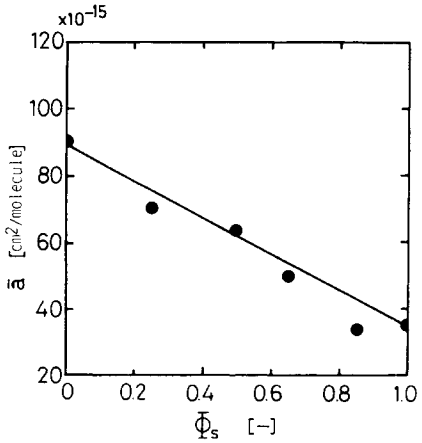

Fig. 1. Adsorption area of NaLS emulsifier molecule, $\bar{a}$, versus average mole fraction of ST units in copolymer particles, Φ_s (condition: room temperature).

cal values (solid line) predicted by Eq. (20c). It is seen that the variation of $\bar{a}$ value with the average copolymer composition of the copolymer particles obeys Eq. (20c) within experimental errors.

Effect of Initiator Concentration

In this kinetic model, only ϵ_I and ϵ are the unknown parameters to be determined, as shown by Eqs. (9′) and (17′). Therefore, the values of ϵ and ϵ_I are determined first as shown below. According to the tentative solution of these kinetic equations, it was found that in the higher range of initial initiator concentration, the calculated values of N_T were uniquely determined only by the value of ϵ_I independently of the value of ϵ, and further that in the lower range of initial initiator concentration, on the contrary, they were determined only by the value of ϵ, independently of the value of ϵ_I and the initial initiator concentration. Based on this characteristic feature, the value of ϵ_I could be easily determined as $\epsilon_I = 2.0 \times 10^{-5}$. Figure 2 shows a comparison between the calculated and experimental values of N_T under the conditions, $M_{os} = M_{om} = 0.10$ g/cm^3 water and $S_o = 6.25$ g/dm^3 water, where in the calculation, the value of ϵ_I as fixed at 2.0×10^{-5} and the value of ϵ was varied. It is seen that in the higher range of initiator concentration, the calculated value of N_T eventually approaches the calculated line corresponding to the values of $\epsilon = 0$ and $\epsilon_I = 2.0 \times 10^{-5}$, regardless of the value of ϵ. It is also seen from this comparison that the value of $\epsilon = 0$ gives best fit between the calculated and experimental values of N_T. Thus, under the condition, $M_{os} = M_{om}$, we have

$$\epsilon_I = 2.0 \times 10^{-5} \quad \text{and} \quad \epsilon = 0 \tag{36}$$

The fact that $\epsilon = 0$ indicates that the desorbed radicals are less effective for particle nucleation than the charged radicals stemmed from the initiator. This differs from the VAC emulsion homopolymerization where VAC radicals are very reactive and hence, the desorbed VAC monomer radicals could also take

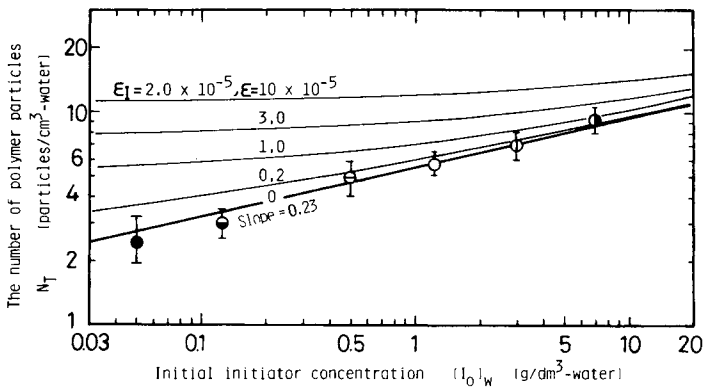

Fig. 2. Determination of ϵ values and comparison between the predicted and observed values of N_T at various concentrations of initiator initially charged, $[I_o]_w$ (conditions: 50°C; $S_o = 6.25$ g/dm^3-water; $M_{os} = M_{om} = 0.10$ g/cm^3-water; I_o(g/dm^3-water) = (◑) 7.0, (◔) 3.0, (○) 1.25, (⊖) 0.50, (◒) 0.125, (●) 0.050).

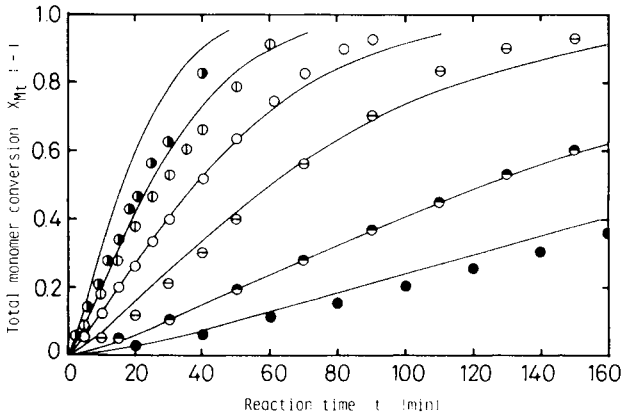

Fig. 3. Comparison between the predicted and observed total monomer conversion versus time histories at various initial initiator concentrations (conditions and keys used are the same as those in Fig. 2).

part in directly forming polymer particles.[13] In Figure 3 the experimental conversion versus time histories are compared with those predicted using $\epsilon_I = 2.0 \times 10^{-5}$ and $\epsilon = 0$. It is seen that the calculated curves agree fairly well with the experimental data points except for the higher range of initial initiator concentrations. The reason for the discrepancy seen at higher initial initiator concentrations may be due to the fact that, in this kinetic model, the radical termination in the aqueous phase is neglected in order to avoid complexity.

Effect of Emulsifier Concentration

Effect of emulsifier concentration initially charged on the number of polymer particles formed and the progress of copolymerization are examined experimentally with the initial initiator concentration and monomer composition fixed, and the experimental results are compared with the theoretical predictions to demonstrate the validity of the values of ϵ_I and ϵ determined above.

Figure 4 shows the effect of emulsifier concentration initially charged on the number of polymer particles produced. It is seen that the number of polymer particles produced attains to a constant value from the very beginning. These constant values of the number of polymer particles are plotted against the initial emulsifier concentration forming micelles, S_{Mo}, (Fig. 5), where the critical micellar concentration, S_{cmc}, is taken as 0.5 g/dm^3 water.[8] The values predicted by calculation using $\epsilon_I = 2.0 \times 10^{-5}$ and $\epsilon = 0$ are also depicted by a solid line. It can be seen from this figure that the calculated values agree very well with those observed in the higher range of emulsifier concentration where particle nucleation from the emulsifier micelles is dominant, while in the vicinity of the CMC, the observed value becomes somewhat higher than that calculated. This will be due to additional particle formation by the so-called homogeneous nucleation mechanism.[14] On the other hand, Figure 6 shows a comparison between the experimental and calculated conversion versus time histories. Furthermore, the observed copolymer compositions are plotted against the total monomer conversion along with the calculated values

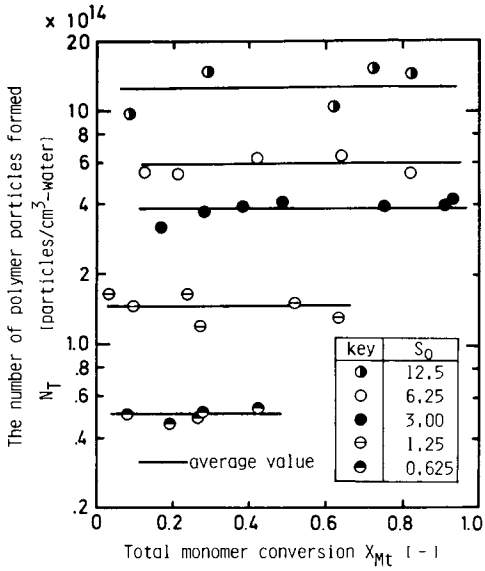

Fig. 4. Effect of initial emulsifier concentration on the number of polymer particles formed (conditions: 50°C; I_o = 1.25 g/dm^3-water; $M_{os} = M_{om}$ = 0.10 g/cm^3-water; S_o (g/dm^3-water) = (◑) 12.5, (○) 6.25, (●) 3.00, (⊖) 1.25, (◓) 0.625).

(solid line) in Figure 7. The experimental data points and the keys shown in Figures 5, 6, and 7 correspond to those in Figure 4. Considering that the experimental data points are in fairly good agreement with the predicted values (solid lines) obtained by using $\epsilon_I = 2.0 \times 10^{-5}$ and $\epsilon = 0$, as can be seen from each of the preceding figures, we can conclude that the kinetic model with the values of $\epsilon_I = 2.0 \times 10^{-5}$ and $\epsilon = 0$ can provide a satisfactory

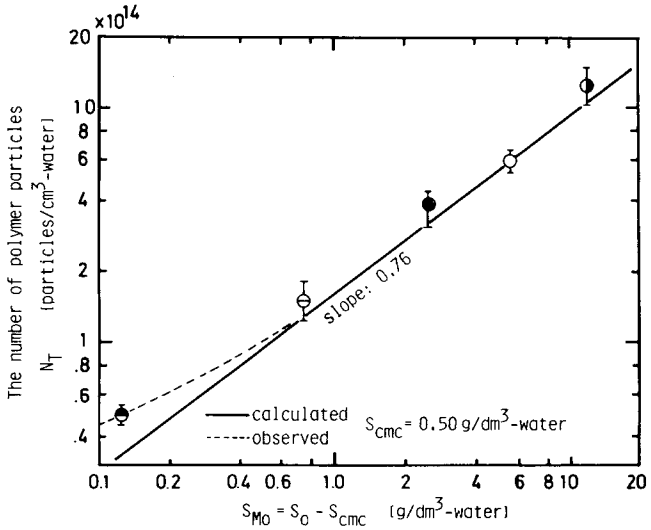

Fig. 5. Comparison between the predicted and observed values of N_T at various initial concentrations of emulsifier forming micelles, S_{Mo} (conditions and keys used are the same as those in Fig. 4).

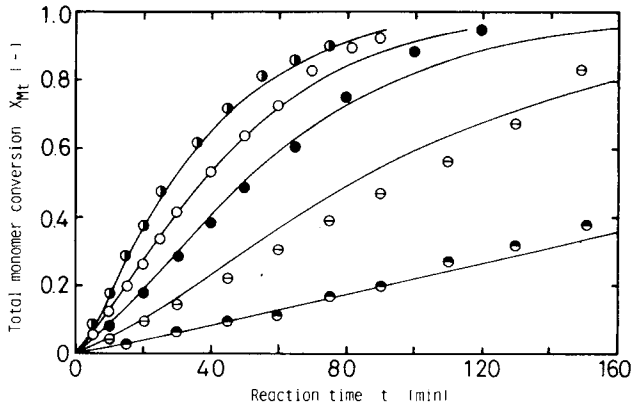

Fig. 6. Comparison between the predicted and observed total monomer conversion versus time histories at various initial emulsifier concentrations (conditions and keys used are the same as those in Fig. 4).

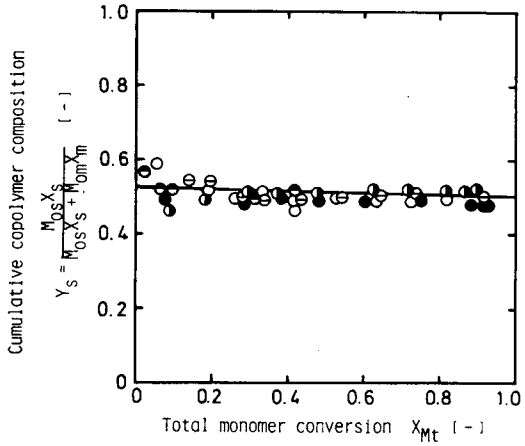

Fig. 7. Comparison between the predicted and observed cumulative copolymer composition, Y_s, versus total monomer conversion curves (conditions and keys used are the same as those in Fig. 4).

explanation of the effect of emulsifier concentration on the kinetic features of the emulsion copolymerization of ST and MMA under the condition, $M_{os} = M_{om}$.

Effect of Monomer Composition

As suggested in the previous section, it is reasonable to consider that the values of ϵ_I and ϵ are influenced by the monomer composition in the interval of particle formation. At the present stage, however, it is not clear how these values depend on the monomer composition, so that we assume as the first approximation that the value of ϵ_I can be expressed by a linear combination of monomer composition and each ϵ value that can describe the particle

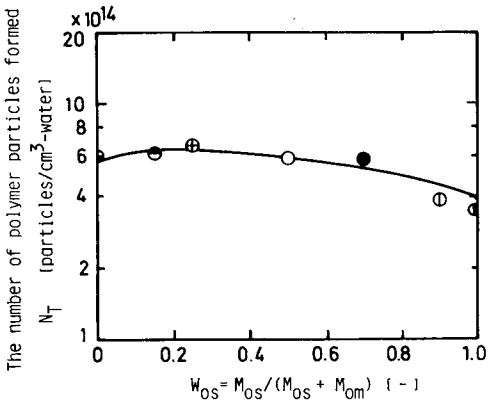

Fig. 8. Comparison between the predicted and observed values of N_T at various comonomer compositions in the initial monomer feed, W_{os}, initial weight fraction of ST monomer (conditions: S_o = 6.25 g/dm^3-water; I_o = 1.25 g/dm^3-water, M_{ot} = 0.20 g/cm^3-water; W_{os} = (◑) 1.0, (⊙) 0.90, (●) 0.70, (○) 0.50, (⊕) 0.25, (◓) 0.15, (◒) 0).

nucleation process in the emulsion homopolymerization of each monomer, although there is no clear theoretical basis for this.

$$\epsilon_I = \epsilon_{Is}F_s + \epsilon_{Im}(1 - F_s) \tag{37}$$

where ϵ_{Is} and ϵ_{Im} are the ϵ values determined for the emulsion homopolymerizations of ST and of MMA, respectively. F_s is the average mole fraction of ST in the micelles during the interval of particle formation and can be approximately taken as the mole fraction of ST in the initial monomer charge, F_{os}, because the interval of particle formation is usually very short compared with the whole polymerization period. The numbers of polymer particles observed in the emulsion homopolymerizations of ST and of MMA are, as shown in Figure 8, 3.8 × 10^{14} and 6.0 × 10^{14} particles/cm^3 water, respectively. For example, the value of ϵ_{Is} can be determined so that the value of N_T calculated for the homopolymerization of ST coincides with 3.8 × 10^{14} particles/cm^3 water. The values of ϵ_{Is} and ϵ_{Im} thus determined are

$$\epsilon_{Is} = 0.83 \times 10^{-5}, \qquad \epsilon_{IM} = 3.3 \times 10^{-5} \tag{38}$$

The value of ϵ_I predicted by calculation using Eqs. (37) and (38) for the conditions in Figure 2 ($M_{os} = M_{om}$ = 0.10 g/cm^3 water) is $\epsilon_I = 2.05 \times 10^{-5}$, and agrees very well with the actual value given by Eq. (36). Therefore, Eq. (37) can be regarded as a satisfactory expression for estimating the value of ϵ_I. In Figure 8, the number of polymer particles predicted by calculation using $\epsilon = 0$ and the value of ϵ_I thus obtained (solid line) and the experimental data points are plotted as a function of the weight fraction of ST in the initial monomer feed. A good agreement can be seen between the experimental and calculated values. Figure 9 shows a comparison between the calculated and experimental conversion versus time histories, corresponding to the experiments shown in Figure 8. It is seen that at lower range of monomer conversion, the calculated lines explain very well the observed data points over the

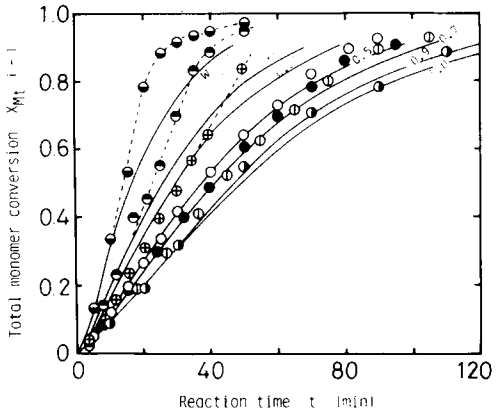

Fig. 9. Comparison between the predicted and observed total monomer conversion versus time histories at various comonomer compositions in the initial monomer feed (conditions and keys used are the same as those in Fig. 8).

whole range of monomer composition but disagreement between them at a higher range of monomer conversion becomes gradually marked with increasing the fraction of MMA monomer in the initial monomer feed. The reason for this may be ascribed to the so-called Trommsdorff "gel" effect, which usually results in an increase in the rate of emulsion polymerization by increasing the number of radicals per particle. The gel effect is apt to take place to a great extent in the emulsion homopolymerization of MMA. However, Figure 10 shows that the copolymer compositions calculated without allowing for the gel effect (solid lines) are in good agreement with the experimental data points in spite of the discrepancy between the calculated and experimental conversions at a higher range of monomer conversion. This means that the instantaneous copolymer composition, y_s, given by Eq. (21) is not affected by the gel effect; that is, that although the rate of copolymerization for each monomer is

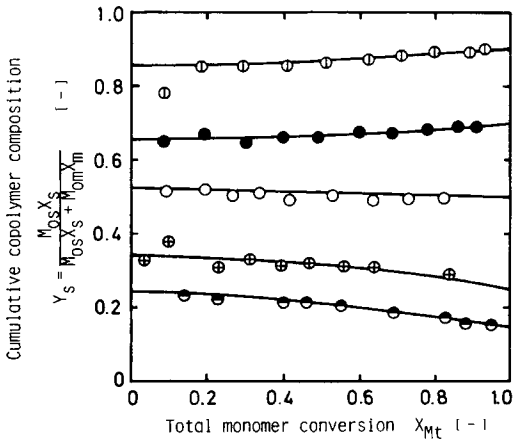

Fig. 10. Comparison between the predicted and observed cumulative copolymer composition, Y_s, versus total monomer conversion curves (conditions and keys used are the same as those in Fig. 8).

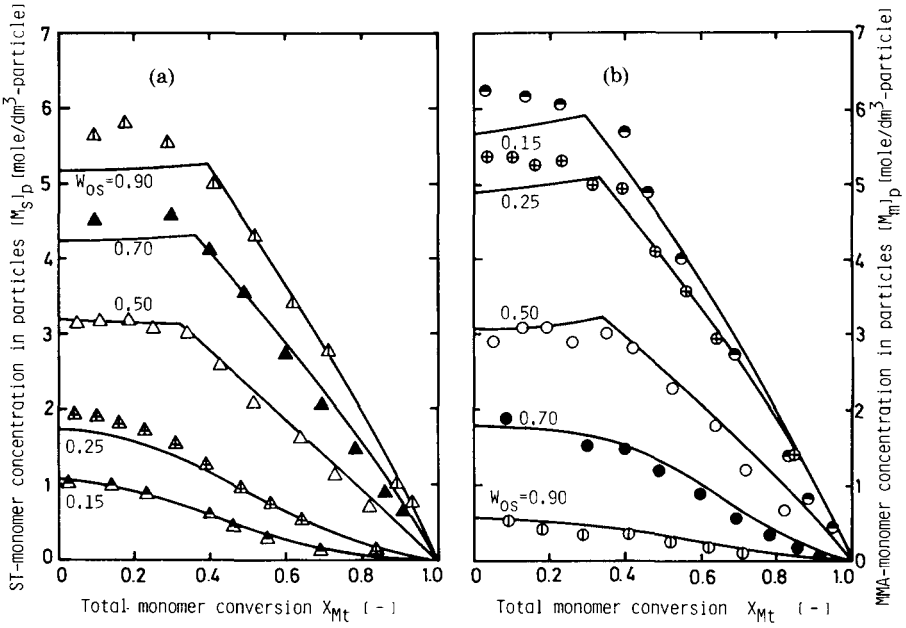

Fig. 11. Comparison between the predicted and observed concentration of each monomer in the polymer particles versus total monomer conversion curves at various comonomer compositions in the initial monomer feed (conditions and keys used in (b) are the same as those in Fig. 8).

accelerated in the presence of the gel effect, the ratio of each copolymerization rate is unaltered. Furthermore, it is seen from Figure 11 that the concentration of each monomer in the polymer particles calculated without taking the gel effect into consideration (solid lines) agrees well with the concentration observed within experimental errors, even in the range where dominant gel effect takes place. The inflection points on the calculated curves correspond to the critical monomer conversions where monomer droplets have just disappeared from the water phase due to complete absorption by the polymer particles. From these findings, we can conclude that Eq. (13) holds even in the presence of dominant gel effect and hence, the relationship between the monomer concentrations in the polymer particles and the total monomer conversion is not affected by the gel effect. It is also concluded from the comparisons given above that the kinetic model developed in this work provides a satisfactory description of the kinetic features affected by the composition of monomer initially charged, except for the rate of copolymerization in the range where the Trommsdorff gel effect is dominant.

SUMMARY AND CONCLUSION

We have proposed a mathematical kinetic model for the unseeded emulsion copolymerization of ST and MMA, based on the conclusion of our previous study that the emulsifier micelle is the principal locus of particle nucleation in this emulsion copolymerization system. In this model, the radicals with and without electric charge were discriminated from each other in view of the role in the process of particle formation. From the comparisons between the

experimental and calculated results, we could obtain an important conclusion that in this system, the polymer particles were generated by the charged radicals stemming from the initiator, while the uncharged radicals in the water phase, which were mainly produced in the polymer particles by chain transfer to monomer followed by desorption into the water phase, did not produce an appreciable number of polymer particles. It should be noted, however, that while these desorbed radicals do not take part in forming particle nuclei in this system, radical desorption from the micelles and the polymer particles indirectly results in an increase in the number of polymer particles produced because radical desorption brings about a decrease in the average volumetric growth rate per particle, which accordingly extends the time period of particle formation.

Recently, it has been proposed by Lichti et al.[15] that coagulation of primary particle is the main factor determining the final number of polymer particles produced. If this is the case in this system, the value of ϵ, which governs the number of polymer particles produced in this reaction model, must depend particularly on the concentration of the emulsifier initially charged. However, the constant value of ϵ was obtained regardless of the concentration of the emulsifier, initiator, and monomers initially charged. This would be a good evidence, although indirect, refuting the claim that coagulation is a dominant factor in this system.

Thus, it can be concluded from the comparisons presented so far that the kinetic model developed here could provide a satisfactory description of the characteristic kinetic features of the unseeded emulsion copolymerization of ST and MMA with sodium lauryl sulfate and potassium persulfate as emulsifier and initiator, respectively, except for the rate of copolymerization in the range where Trommsdorff gel effect is predominant.

References

1. M. Nomura, M. Kubo, and K. Fujita, *Mem. Fac. Eng. Fukui Univ.*, **29**, (2), 167 (1981).
2. M. Nomura, K. Yamamoto, I. Horie, and K. Fujita, *J. Appl. Polym. Sci.*, **27**, 2483 (1983).
3. M. Nomura, M. Kubo, and K. Fujita, *J. Appl. Polym. Sci.*, **28**, 2767 (1983).
4. M. Nomura and K. Fujita, *Makromol. Chem., Suppl.*, **10 / 11**, 25 (1985).
5. C. C. Lin, H. C. Ku, and W. Y. Chiu, *J. Appl. Polym. Sci.*, **26**, 1327 (1981).
6. G. Storti, M. Albano, M. Morbideli, and S. Carra, *Polymer Reaction Engineering*, K.-H. Reichert and W. Geiseler, Eds., Huthig & Wepf, Heidelberg, 1986, p. 165.
7. M. Nomura, Y. Kouno, and K. Fujita, *J. Polym. Sci. Polym. Let. Ed.* **26**, 385 (1988).
8. M. Harada, M. Nomura, H. Kojima, W. Eguchi, and S. Nagata, *J. Appl. Polym. Sci.*, **16**, 811 (1972).
9. (a) J. Ugelstad, P. C. Mørk, P. Dahl, and P. Ranges, *J. Polym. Sci.*, Part C, **27**, 49 (1969); (b) M. Harada, M. Nomura, W. Eguchi, and S. Nagata, *J. Chem. Eng. Jpn.* **4**, 54 (1971).
10. F. K. Hansen and J. Ugelstad, in *Emulsion Polymerization*, I. Piirma Ed., Academic Press, New York, 1982, Chap. 2.
11. M. Morton, S. Kaizermann, and M. W. Altier, *J. Colloid Sci.*, **9**, 300 (1954).
12. J. Guillot, *Makromol. Chem., Rapid Comm.*, **1**, 697 (1980).
13. M. Nomura, M. Harada, M. Eguchi, and S. Nagata, *Am. Chem. Soc. Symp. Ser.*, **24**, p. 102 (1976).
14. R. Fitch, *Am. Chem. Soc. Symp. Ser.*, **165**, 1 (1981).
15. G. Lichti, R. G. Robert, and D. H. Napper, *J. Polym. Sci., Polm. Chem. Ed.*, **21**, 269 (1983).

Received October 1, 1987
Accepted January 7, 1988